Orbital-order melting in rare-earth manganites: Role of superexchange

Andreas Flesch,[1] Guoren Zhang,[1] Erik Koch,[2] and Eva Pavarini[1,*]

[1]*Institute for Advanced Simulation and JARA, Forschungszentrum Jülich, 52425 Jülich, Germany*

[2]*German Research School for Simulation Sciences, 52425 Jülich, Germany*

(Received 4 November 2011; revised manuscript received 10 January 2012; published 26 January 2012)

We study the mechanism of orbital-order melting observed at temperature T_{OO} in the series of rare-earth manganites. We find that the purely electronic many-body super-exchange mechanism yields a transition temperature T_{KK} that decreases with decreasing rare-earth radius and increases with pressure, opposite to the experimental T_{OO}. We show that the tetragonal crystal-field splitting reduces T_{KK} further increasing the discrepancies with experiments. This proves that super-exchange effects, although very efficient, in the light of experimentally observed trends play a minor role for the melting of orbital ordering in rare-earth manganites.

DOI: 10.1103/PhysRevB.85.035124 PACS number(s): 71.27.+a, 75.25.Dk, 71.30.+h, 71.28.+d

I. INTRODUCTION

The role of orbital degrees of freedom[1] in the physics of $LaMnO_3$, and in particular the cooperative Jahn-Teller transition, has long been debated.[1–5] *Ab initio* LDA + U calculations show that Coulomb repulsion effects are key to understanding the orbitally ordered antiferromagnetic ground state.[4] The purely electronic super-exchange mechanism alone, however, is not sufficient[6] to explain the presence of cooperative Jahn-Teller distortions in nanoclusters up to $T \sim 1150$ K[7,8] (orbitally disordered phase). Still, super-exchange effects are rather large: T_{KK}, the temperature at which super-exchange alone, i.e., in the absence of static Jahn-Teller distortions due to electron-phonon coupling, would drive the transition is remarkably close to T_{OO}, the temperature at which the cooperative Jahn-Teller distortion disappears in resonant x-ray and neutron scattering.[9] This fact could indicate that super-exchange, although insufficient to explain the persistence of Jahn-Teller distortions in the orbitally disordered phase, plays a major role in the orbital order-to-disorder transition (orbital order melting) observed at T_{OO}. Here we resolve this issue.

Remarkably, orbital-order melting has been observed[10–12] in the full series of orthorhombic rare-earth (RE) manganites, $REMnO_3$. These systems are perovskites (Fig. 1) with electronic configuration Mn $3d^4$ ($t_{2g}^3 e_g^1$). In the cooperative Jahn-Teller phase ($T < T_{OO}$), the MnO_6 octahedra are tilted and rotated and exhibit a sizable Jahn-Teller distortion with long and short MnO bonds antiferro-ordered in the xy plane and ferro-ordered along **z**. Neutron and x-ray diffraction data show that T_{OO} increases from 750 to ∼1500 K with decreasing ionic radius IR (La → Dy);[9–12] under increasing pressure eventually orbital order melts,[13,14] while Jahn-Teller distortions still persist in nanoclusters.[8]

The strength of super-exchange is directly linked to the amplitude of the hopping integrals, which depend on the cell volume and distortions.[15,16] In the $REMnO_3$ series the volume decreases with ionic radius. Tilting and rotation, however, increase, because of the increasing mismatch between the Mn-O and RE-O bond lengths. For $LaMnO_3$ a volume collapse at T_{OO} has been reported.[17] Under pressure, up to $P = 18$ GPa the volume decreases by ∼10%, while tilting or rotation slightly decreases. A sizable volume reduction typically increases the Mn-O hopping integrals, while tilting and rotation tend to reduce them, reducing super-exchange effects. The scenario is further complicated by the local crystal field,[6,18,19] which can, depending on its size and symmetry, help or compete with super-exchange, and thus even reverse the trends.

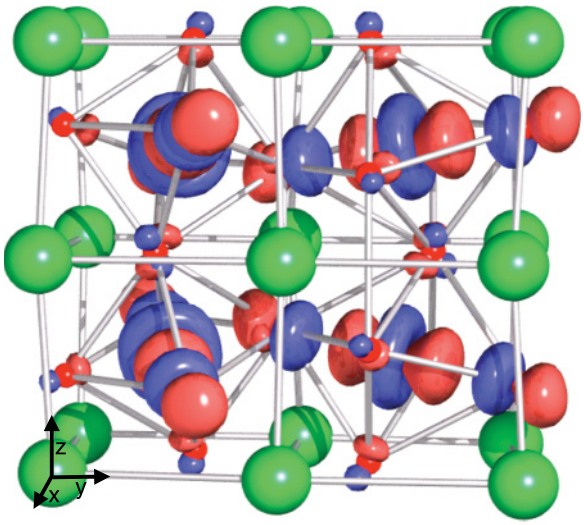

FIG. 1. (Color online) Orbital order in $TbMnO_3$, as obtained by LDA+DMFT calculations. The pseudocubic axes pointing along Mn-Mn bonds are shown in the left corner.

In this work we clarify the role of the purely electronic super-exchange mechanism in orbital-order melting. To do this, we perform *ab initio* calculations based on the local density approximation (LDA) + dynamical mean-field theory (DMFT) method[20] in the paramagnetic phase for fixed atomic position, explicitly setting to zero the static Jahn-Teller crystal-field splitting ε_{JT}, and excluding the effect of phonons. Apart from ε_{JT}, a tetragonal crystal-field splitting ε_T is present. We show that, in the absence of such crystal-field splitting, while in $LaMnO_3$ $T_{KK} \sim T_{OO}$, in all other systems T_{KK} is 2–3 times smaller than T_{OO}. Thus, while T_{OO} strongly increases with decreasing ionic radius, T_{KK} slightly decreases. Taking the tetragonal splitting into account, these trends are enhanced even further. This proves that, although very large, in view of the reported experimental trends, super-exchange plays a minor role in the orbital-melting transition.

II. MODEL AND METHOD

The minimal model Hamiltonian to study super-exchange effects in manganites is the Hubbard model for the e_g bands in the magnetic field $h = J S_{t_{2g}}$ of disordered t_{2g} spins $\mathbf{S}_{t_{2g}}$:[21]

$$H = \sum_i \varepsilon_{\rm JT}\tau_{ix} + \varepsilon_T \tau_{iz} \sum_{i\neq i' m\sigma m'\sigma'} t^{i,i'}_{m,m'} u^{i,i'}_{\sigma,\sigma'} c^\dagger_{im\sigma} c_{i'm'\sigma'} - h\sum_{im}(n_{im\Uparrow} - n_{im\Downarrow}) + U\sum_{im} n_{im\Uparrow} n_{im\Downarrow} + \frac{1}{2}\sum_{im\neq m'\sigma\sigma'} (U - 2J - J\delta_{\sigma,\sigma'}) n_{im\sigma} n_{im'\sigma'} . \quad (1)$$

Here $c^\dagger_{im\sigma}$ creates an electron with spin $\sigma = \Uparrow, \Downarrow$ in a Wannier orbital $|m\rangle = |x^2 - y^2\rangle$ or $|3z^2 - r^2\rangle$ at site i, and $n_{im\sigma} = c^\dagger_{im\sigma} c_{im\sigma}$. $\Uparrow$ ($\Downarrow$) indicates the e_g spin parallel (antiparallel) to the t_{2g} spins (on that site). In the paramagnetic state, the matrix u ($u^{i,i'}_{\sigma,\sigma'} = 2/3$) accounts for the orientational disorder of the t_{2g} spins;[21] $t^{i,i'}_{m,m'}$ is the LDA[15] hopping integral from orbital m on site i to orbital m' on site $i' \neq i$, obtained *ab initio* by downfolding the LDA bands and constructing a localized e_g Wannier basis. The on-site term $\varepsilon_{\rm JT}\tau_{ix} + \varepsilon_T\tau_{iz}$ yields the LDA crystal-field matrix. It is the sum of a Jahn-Teller ($\varepsilon_{\rm JT}\tau_{ix}$) and a tetragonal ($\varepsilon_T\tau_{iz}$) term, where τ_{ix} and τ_{iz} are the pseudospin-1/2 operators $\tau_{ix} = \frac{1}{2}\sum_{\sigma,m\neq m'} c^\dagger_{im\sigma} c_{im'\sigma}$, $\tau_{iz} = \frac{1}{2}\sum_{\sigma,m}(-1)^{\delta_{m,x^2-y^2}} c^\dagger_{im\sigma} c_{im\sigma}$. U and J are the direct and exchange screened on-site Coulomb interaction. We use the theoretical estimates $J = 0.75$ eV, $U \sim 5$ eV (see Refs. 6, 22, and 23) and $2JS_{t_{2g}} \sim 2.7$ eV;[23] we find that, in the high-spin regime, $T_{\rm KK}$ is not sensitive to the specific value of $2JS_{t_{2g}}$, and therefore we keep h fixed in all results we present. We solve (1) within dynamical mean-field theory[24] using a quantum Monte Carlo[25] (QMC) solver, working with the full self-energy matrix $\Sigma_{mm'}$ in orbital space and a 4 Mn supercell with the Pbnm space group;[15,19] this ensures that we properly account for the point symmetries and the essential $\mathbf{k}$ dependence.[26] We construct the LDA Wannier functions via the downfolding procedure based on the Nth-Order Muffin-Tin (NMTO) method.[15] Additionally, we perform calculations based on the Linearized Augmented Plane Wave approach (LAPW)[27] and construct maximally localized Wannier functions following the Marzari-Vanderbilt procedure.[28] The band structures and parameter trends obtained with the two methods are very similar.[29]

To determine the super-exchange transition temperature $T_{\rm KK}$ we use two independent approaches. In the first, we calculate the order parameter p as a function of temperature T (Fig. 2, bottom); in the second we calculate the $T = 0$ total energy gain $\Delta E_{\rm KK}$ (Fig. 2, top) due to orbital order. To disentangle the effects of super-exchange from those of the static Jahn-Teller crystal field we perform the calculations for $\varepsilon_{\rm JT} = 0$.

In the first approach, the order parameter for orbital ordering is the orbital polarization $p \equiv |n_1 - n_2|$, where $|1\rangle$ and $|2\rangle$ are the natural orbitals,[31] i.e., the eigenvectors of the density matrix in e_g space.[32] To determine the trends in $T_{\rm KK}$ we calculate $p = p(T)$ for all materials in the series. They differ in (i) hopping integrals and (ii) crystal field, due to static distortions.[33] We calculate p for the real system ($H^{\rm LDA}$),

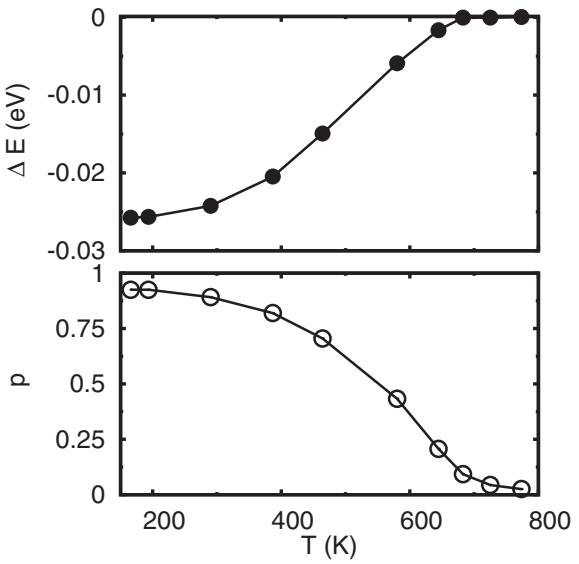

FIG. 2. Top: Energy gain per formula unit due to orbital polarization, $\Delta E[p(T)] = \Delta E(T)$, in the case of $LaMnO_3$. Error bars are smaller than the symbols. Bottom: Order parameter (orbital polarization) $p(T)$ vs temperature.

for ideal structures with the same hopping integrals but no crystal field, $\varepsilon_T = \varepsilon_{\rm JT} = 0$ (Fig. 3), and for ideal structures with only tetragonal splitting, $\varepsilon_{\rm JT} = 0$ (Fig. 4). As expected for an order parameter, in the absence of a crystal field, $p(T) \approx 0$ for $T > T_{\rm KK}$ while $p(T \to 0) = 1$ (see Fig. 2); $T_{\rm KK}$ obtained from $p(T)$ in the absence of a crystal field is shown in Fig. 3. In the presence of a finite tetragonal crystal field ($\varepsilon_T \gtrsim 100$ meV), the orbital polarization $p(T)$ is finite and sizable even above 1200 K, but the most occupied natural orbital, $|\theta\rangle = -\sin\frac{\theta}{2}|x^2 - y^2\rangle + \cos\frac{\theta}{2}|3z^2 - r^2\rangle$, suddenly changes as the temperature approaches the critical temperature $T^{\varepsilon_T}_{\rm KK}$; the rotation of $|\theta\rangle$ with temperature is shown in Fig. 4.

In the second approach we obtain the energy gain due to orbital order from the difference in total energy between

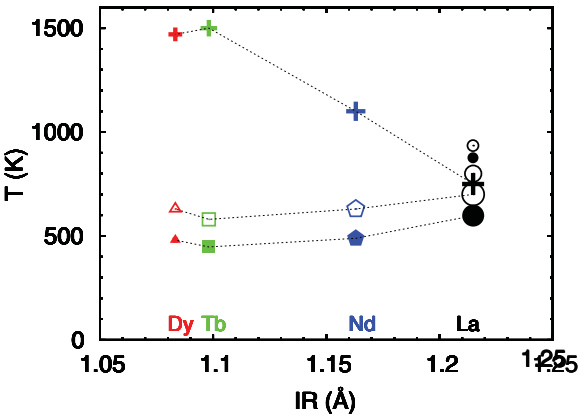

FIG. 3. (Color online) Orbital-order transition temperature $T_{\rm KK}$[30] vs RE^{3+} radius in the $REMnO_3$ series, with RE = Dy (triangles), Tb (squares), Nd (pentagons), La (circles). Full (empty) symbols: $T_{\rm KK}$ from LDA + DMFT total-energy (order parameter) calculations. Symbols of decreasing size: $P = 0$, 5.4, and 9.87 GPa. Crosses: Experimental values (ambient pressure) from Refs. 10–12.

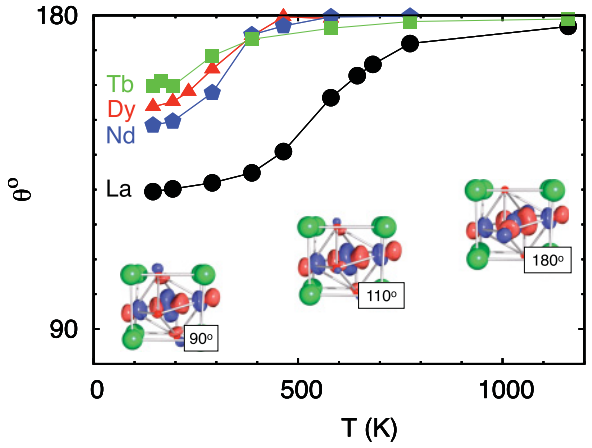

FIG. 4. (Color online) Rotation of the most occupied state $|\theta\rangle$ as a function of temperature in the presence of a 130 meV tetragonal crystal field. The orbitals are shown for $TbMnO_3$. The most occupied orbital remains well defined in the full temperature range; the orbital polarization is merely reduced by 30% at ∼800 K.

the orbitally polarized and the orbitally disordered states, in the absence of crystal fields ($\varepsilon_T = \varepsilon_{JT} = 0$). We first perform LDA+DMFT calculations for decreasing temperature and calculate the total energy per formula unit at temperature T and polarization $p = p(T)$, $E_{TOT}(p)$. Next, we repeat the same procedure, but with the constraint $p = 0$ ($\Sigma_{1,1} = \Sigma_{2,2}$ and $\Sigma_{1,2} = 0$).

The total energy is given by[34]

$$E_{TOT}(p) = E^{LDA}_{TOT} + \langle H\rangle_p - E^{LDA}_{e_g} - E_{DC}.$$

Here E^{LDA}_{TOT} is the LDA total energy; $E^{LDA}_{e_g}$ is the thermal average of (1) in the noninteracting limit ($U = J = 0$),

$$E^{LDA}_{e_g} = \frac{1}{\beta}\frac{1}{N_{\mathbf{k}}}\sum_{\mathbf{k}n} \mathrm{Tr}\left[H^{LDA}_{\mathbf{k}} G^{LDA}_{\mathbf{k}}(i\omega_n)\right] e^{i\omega_n 0^+},$$

where $H^{LDA}_{\mathbf{k}}$ is the noninteracting part of (1), $G^{LDA}_{\mathbf{k}}$ is the corresponding noninteracting Green-function matrix, ω_n are Fermionic Matsubara frequencies, and $\beta = k_B T$; $\langle H\rangle_p$ is the actual thermal average of (1) for polarization $p(T)$; finally, E_{DC} is the double-counting correction, which subtracts the correlation energy already contained in the LDA total energy. Since E^{LDA}_{TOT}, $E^{LDA}_{e_g}$ and E_{DC} do not depend on the constraint $p = 0$, only $\langle H\rangle_p$ contributes to the energy difference

$$\Delta E(p) = E_{TOT}(p) - E_{TOT}(0) = \langle H\rangle_p - \langle H\rangle_{p=0}. \quad (2)$$

$\langle H\rangle_p$ can be split[34] into a single-electron contribution [from the first three terms in (1)], and a correlation contribution [from the last two terms in (1)]. We evaluate the single-electron contribution as $E^{LDA}_{e_g}$, however, with $G^{LDA}_{\mathbf{k}}(i\omega_n)$ replaced by the full Green-function matrix including the self-energy matrix. We obtain the correlation term with QMC from the double-occupancy matrix. Since $-\Delta E_{TOT}(p) \sim 10-50$ meV, error bars, in particular the QMC statistical error on the double-occupancies matrix, have to be controlled to high accuracy.[35]

The total-energy gain for $LaMnO_3$ is shown in Fig. 2. We obtain similar behavior for the other systems. While in the constrained calculations, by construction, $p = 0$ in the full temperature range, the unconstrained calculations yield finite p below T_{KK}; the polarization reaches its maximum value in the zero-temperature limit. Thus, in the zero-temperature limit, we can extrapolate from $\Delta E(p)$ the super-exchange energy gain due to orbital polarization, $\Delta E_{KK} = E_{TOT}(p = 1) - E_{TOT}(p = 0)$.

III. RESULTS

Remarkably, we find that the static mean-field[36] relation $T_{KK} \equiv |2\Delta E_{KK}|/k_B$, which is valid for a spin-1/2 Heisenberg-like model[1] with arbitrary coupling constants, gives transition temperatures close to those obtained from order-parameter calculations, the difference being a mere small shift.[37] Our results are shown in Fig. 3. While $T_{KK} \sim T_{OO}$ in $LaMnO_3$, in all other systems T_{KK} is a factor 2–3 smaller than the experimental estimate for T_{OO}. Moreover, T_{KK} is maximum in $LaMnO_3$ and roughly decreases with ionic radius from RE = La to Tb, and then increases again. T_{KK} also increases under pressure. These trends are opposite to those reported experimentally for the orbital melting temperature.[26] They can be ascribed to the increasing distortions along the $REMnO_3$ series, and the decrease in volume and tilting or rotation with increasing pressure. Finally, for all systems super-exchange favors the occupation of the orbital (signs are given for the site displayed in Fig. 4) $|\theta\rangle = -\sin\frac{\theta}{2}|x^2 - y^2\rangle + \cos\frac{\theta}{2}|3z^2 - r^2\rangle$, with $\theta = 90°$, while experimentally $\theta \sim 108°$ in $LaMnO_3$ increasing with decreasing ionic radius to 114° in $TbMnO_3$.[38]

Due to the competition between the tetragonal crystal-field splitting ε_T and super-exchange (which favor the occupation of different orbitals), T_{KK} is reduced[42] even further. We find that for finite ε_T the system is orbitally ordered already at high temperature due to the crystal field, but the occupied orbital has $\theta = 180°$. In Fig. 4 we show the results for ε_T fixed at ∼130 meV, sizable but smaller than for any of the considered systems (see Fig. 5). We find that at the reduced critical temperature $T^{\varepsilon_T}_{KK}$, super-exchange rotates the orbital toward 90°. The change in T_{KK} is small for $LaMnO_3$, but

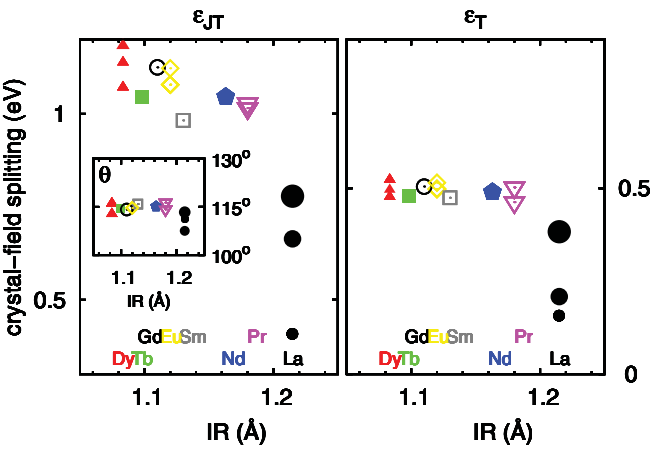

FIG. 5. (Color online) Evolution of the crystal field with the RE^{3+} radius (structural data from Refs. 11, 39–41). Filled circles of decreasing size: $LaMnO_3$ for $P = 0$, 5.4, and 9.87 GPa.[13] Inset: Calculated occupied orbital.

T_{KK} is reduced to 400 K for $NdMnO_3$, and even more for $DyMnO_3$ and $TbMnO_3$. Furthermore, in the zero-temperature limit, the smaller $T_{KK}^{\varepsilon_T}$, the closer is θ to 180°. Thus a fixed $\varepsilon_T \sim 130$ meV enhances the trend found for $\varepsilon_T = 0$: T_{KK} is larger in $LaMnO_3$ and decreases going to $DyMnO_3$. Still, even for $LaMnO_3$, θ is significantly larger than the experimental 108°. This means that a Jahn-Teller crystal-field splitting ε_{JT} is necessary to explain the experimental θ; Fig. 4 shows that such splitting has to increase for the series RE = La, Nd, Dy, Tb. Taking into account that tetragonal splitting actually increases with decreasing pressure, and substituting La with Nd, Tb, or Dy (Fig. 5), this trend is enhanced even more. For ε_T corresponding to the real structures, down to 150 K we find no super-exchange transition for all systems but $LaMnO_3$. These results can be understood qualitatively in static mean-field theory. In the simplest case, super-exchange yields just an effective Jahn-Teller splitting $\varepsilon_{KK} = \langle \tau_x \rangle \lambda_{KK}$, where λ_{KK} is the molecular field parameter; the self-consistency condition for orbital order is

$$\langle \tau_x \rangle = \tfrac{1}{2} \sin\theta \tanh\left(\beta \sqrt{\varepsilon_T^2 + \varepsilon_{KK}^2}/2\right),$$

with $\sin\theta = \varepsilon_{KK}/\sqrt{\varepsilon_T^2 + \varepsilon_{KK}^2}$. This equation has a nontrivial solution ($\theta \neq 180°$) only if $\lambda_{KK}/2 > \varepsilon_T$. The critical temperature is

$$T_{KK}^{\varepsilon_T}/T_{KK}^0 = \left(\varepsilon_T/2k_B T_{KK}^0\right)/\tanh^{-1}\left(\varepsilon_T/2k_B T_{KK}^0\right),$$

with $k_B T_{KK}^0 = \lambda_{KK}/4$; it decreases with increasing ε_T, while $\theta \to 180°$.[43] For large enough ε_T ($\varepsilon_T > \lambda_{KK}/2$) there is no super-exchange driven transition at all.

IV. CONCLUSIONS

For the orbital-melting transition in rare-earth manganites $REMnO_3$, we find that many-body super-exchange yields a transition temperature T_{KK} very close to T_{OO} only in $LaMnO_3$, while in all other systems T_{KK} is less than half T_{OO}. Moreover, we find that a tetragonal splitting ε_T reduces T_{KK} even further; ε_T increases when La is substituted with Nd, Tb, or Dy and decreases under pressure, further enhancing the discrepancy with experiments. Finally, super-exchange effects become larger with increasing pressure, while experimentally orbital order eventually melts.[13,14] Our work thus proves that, in the light of the experimentally observed trends, super-exchange plays a minor role in the orbital-melting transitions of rare-earth manganites.

ACKNOWLEDGMENTS

We thank I. Loa and K. Syassen for sharing unpublished data. Calculations were done on the Jülich Blue Gene/P and Juropa. We acknowledge financial support from the Deutsche Forschungsgemeinschaft through research unit FOR1346.

*e.pavarini@fz-juelich.de

[1] K. I. Kugel and D. I. Khomskii, Zh. Eksp. Teor. Fiz. **64**, 1429 (1973) [Sov. Phys. JETP **37**, 725 (1973)].
[2] J. B. Goodenough, Phys. Rev. **100**, 564 (1955); J. Kanamori, J. Appl. Phys. Supp. **31**, S14 (1960).
[3] Y. Tokura and N. Nagaosa, Science **288**, 462 (2000); S.-W. Cheong, Nat. Mater. **6**, 927 (2007); E. Dagotto and Y. Tokura, MRS Bull. **33**, 1037 (2008); M. Imada, A. Fujimori, and Y. Tokura, Rev. Mod. Phys. **70**, 1039 (1998).
[4] W.-G. Yin, D. Volja, and W. Ku, Phys. Rev. Lett. **96**, 116405 (2006).
[5] D. Feinberg, P. Germain, M. Grilli, and G. Seibold, Phys. Rev. B **57**, R5583 (1998); C. Lin and A. J. Millis, *ibid.* **78**, 174419 (2008).
[6] E. Pavarini, E. Koch, and A. I. Lichtenstein, Phys. Rev. Lett. **101**, 266405 (2008); E. Pavarini and E. Koch, *ibid.* **104**, 086402 (2010).
[7] M. C. Sánchez, G. Subías, J. García, and J. Blasco, Phys. Rev. Lett. **90**, 045503 (2003); X. Qiu, T. Proffen, J. F. Mitchell, and S. J. L. Billinge, *ibid.* **94**, 177203 (2005); A. Sartbaeva, S. A. Wells, M. F. Thorpe, E. S. Bozin, and S. J. L. Billinge, *ibid.* **99**, 155503 (2007).
[8] A. Y. Ramos, H. C. N. Tolentino, N. M. Souza-Neto, J.-P. Itié, L. Morales, and A. Caneiro, Phys. Rev. B **75**, 052103 (2007); M. Baldini, V. V. Struzhkin, A. F. Goncharov, P. Postorino, and W. L. Mao, Phys. Rev. Lett. **106**, 066402 (2011).
[9] J. Rodríguez-Carvajal, M. Hennion, F. Moussa, A. H. Moudden, L. Pinsard, and A. Revcolevschi, Phys. Rev. B **57**, R3189 (1998); Y. Murakami, J. P. Hill, D. Gibbs, M. Blume, I. Koyama, M. Tanaka, H. Kawata, T. Arima, Y. Tokura, K. Hirota, and Y. Endoh, Phys. Rev. Lett. **81**, 582 (1998).
[10] J.-S. Zhou and J. B. Goodenough, Phys. Rev. B **68**, 144406 (2003); Phys. Rev. Lett. **96**, 247202 (2006).
[11] B. Dabrovski, S. Kolesnika, A. Baszczukb, O. Chmaissema, T. Maxwella, and J. Mais, J. Solid State Chem. **178**, 629 (2005).
[12] G. Maris, V. Volotchaev, and T. T. M. Palstra, New. J. Phys. **6**, 153 (2004).
[13] I. Loa, P. Adler, A. Grzechnik, K. Syassen, U. Schwarz, M. Hanfland, G. K. Rozenberg, P. Gorodetsky, and M. P. Pasternak, Phys. Rev. Lett. **87**, 125501 (2001); I. Loa and K. Syassen (private communication).
[14] J. M. Chen *et al.*, Phys. Rev. B **79**, 165110 (2009).
[15] See E. Pavarini, A. Yamasaki, J. Nuss, and O. K. Andersen, New J. Phys. **7**, 188 (2005).
[16] E. Pavarini, S. C. Tarantino, T. B. Ballaran, M. Zema, P. Ghigna, and P. Carretta, Phys. Rev. B **77**, 014425 (2008).
[17] T. Maitra, P. Thalmeier, and T. Chatterji, Phys. Rev. B **69**, 132417 (2004).
[18] E. Gorelov, M. Karolak, T. O. Wehling, F. Lechermann, A. I. Lichtenstein, and E. Pavarini, Phys. Rev. Lett. **104**, 226401 (2010); M. Malvestuto, E. Carleschi, R. Fittipaldi, E. Gorelov, E. Pavarini, M. Cuoco, Y. Maeno, F. Parmigiani, and A. Vecchione, Phys. Rev. B **83**, 165121 (2011).
[19] E. Pavarini, S. Biermann, A. Poteryaev, A. I. Lichtenstein, A. Georges, and O. K. Andersen, Phys. Rev. Lett. **92**, 176403 (2004).
[20] V. Anisimov, A. Poteryaev, M. Korontin, A. Anohkin, and G. Kotliar, J. Phys. Condens. Matter **9**, 7359 (1997); A. I. Lichtenstein and M. I. Katsnelson, Phys. Rev. B **57**, 6884 (1998).
[21] K. H. Ahn and A. J. Millis, Phys. Rev. B **61**, 13545 (2000). In the high-spin regime the orbital superexchange coupling depends weakly on $u_{\sigma,-\sigma}$ terms;[6] thus we neglect them.

[22]T. Mizokawa and A. Fujimori, Phys. Rev. B **54**, 5368 (1996).
[23]A. Yamasaki, M. Feldbacher, Y.-F. Yang, O. K. Andersen, and K. Held, Phys. Rev. Lett. **96**, 166401 (2006).
[24]A. Georges, G. Kotliar, W. Kraut, and M. J. Rozenberg, Rev. Mod. Phys. **68**, 13 (1996).
[25]J. E. Hirsch and R. M. Fye, Phys. Rev. Lett. **56**, 2521 (1986).
[26]Spatial fluctuations beyond mean-field would just decrease $T_{\rm KK}$, supporting our conclusions even further. Cluster DMFT calculations (see Refs. 6) indicate that, in the case of manganites, the reduction of $T_{\rm KK}$ is actually small.
[27]P. Blaha, K. Schwarz, G. Madsen, D. Kvasnicka, and J. Luitz, WIEN2k, Karlheinz Schwarz, Techn. Universität Wien, Austria, 2001.
[28]A. A. Mostofi, J. R. Yates, Y.-S. Lee, I. Souza, D. Vanderbilt, and N. Marzari, Comput. Phys. Commun. **178**, 685 (2008); J. Kunes, R. Arita, P. Wissgott, A. Toschi, H. Ikeda, and K. Held, *ibid.* **181**, 1888 (2010).
[29]$LaMnO_3$: $\varepsilon_T \sim 350$ meV, $\varepsilon_{\rm JT} = 650$ meV, $t^{001}_{3z^2-r^2,3z^2-r^2} = 392$ meV. $TbMnO_3$: $\varepsilon_T \sim 580$ meV, $\varepsilon_{\rm JT} = 1060$ meV, $t^{001}_{3z^2-r^2,3z^2-r^2} = 349$ meV. See Fig. 5 for comparison with NMTO results; e_g bandwidth differences are ~ 0.1 eV.
[30]All results shown are for $U = 5$ eV and $J = 0.75$ eV. For $P = 9.87$ GPa, setting $\varepsilon_T = \varepsilon_{\rm JT} = 0$ we obtain, however, a metallic solution with $p = 0$. Since $T_{\rm KK}$ decreases with U roughly as $\sim 1/U$, as expected from super-exchange theory, to compare values for constant U, we can extrapolate the $U = 5$ eV value of $T_{\rm KK}$ from the insulating state obtained for slightly larger U ($U = 5.5$ eV, $U = 6$ eV).
[31]P.-O. Löwdin, Phys. Rev. **97**, 1474 (1954).
[32]The orbital polarization p is the analog of the spin polarization $m = n_\uparrow - n_\downarrow$ in a magnetic phase transition.
[33]$\varepsilon_{\rm JT}$ is the only parameter that exhibits a strong T dependence across $T_{\rm OO}$: It goes to zero at $T = T_{\rm OO}$. To single out the effect of super-exchange we set $\varepsilon_{\rm JT} = 0$, and so such T dependence plays no role for the present investigation.
[34]A. K. McMahan, K. Held, and R. T. Scalettar, Phys. Rev. B **67**, 075108 (2003); B. Amadon, S. Biermann, A. Georges, and F. Aryasetiawan, Phys. Rev. Lett. **96**, 066402 (2006); I. Leonov, N. Binggeli, Dm. Korotin, V. I. Anisimov, N. Stojic, and D. Vollhardt, *ibid.* **101**, 096405 (2008).
[35]A simple estimate from the average correlation energy, $\frac{1}{2}Un_{e_g}(n_{e_g} - 1)$, is $\frac{1}{2}[U(2n_{\rm e_g} - 1)]\delta n_{\rm e_g} \ll \Delta E(p)$, which for $\Delta E(p) \sim -10$ meV, $n_{\rm e_g} = 1$ and $U = 5$ eV, yields $\delta n_{e_g} \ll 4 \times 10^{-3}$.
[36]W. Nolting and A. Ramakanth, *Quantum Theory of Magnetism* (Springer, Heidelberg, 2009), p. 306.
[37]Such an overall shift, the same for all materials, merely corresponds to a modified prefactor (e.g., geometrical) in the mean-field expression of $T_{\rm KK}$ vs energy gain with respect to the spin-1/2 Heisenberg model.
[38]M. W. Kim, S. J. Moon, J. H. Jung, J. Yu, S. Parashar, P. Murugavel, J. H. Lee, and T. W. Noh, Phys. Rev. Lett. **96**, 247205 (2006).
[39]J. A. Alonso, M. J. Martinez-Lope, and M. T. Casais, Inorg. Chem. **39**, 917 (2000).
[40]T. Mori, N. Kamegashira, K. Aoki, T. Shishido, and T. Fukuda, Mat. Lett. **54**, 238 (2002).
[41]K. Uusi-Esko, J. Malm, N. Imamura, H. Yamauchi, and M. Karppinen, Mater. Chem. Phys. **112**, 1029 (2008).
[42]E. Pavarini and L. C. Andreani, Phys. Rev. Lett. **77**, 2762 (1996). A similar effect is observed in the two-channel Kondo model; a ferromagnetic channel does not destroy the Kondo effect, but reduces the Kondo temperature.
[43]The energy gain due to the pseudospin rotation is $2|\Delta E|/k_B T^{\varepsilon_T}_{\rm KK} = (1-x)^2(\tanh^{-1} x)/x$, where $x = 2\varepsilon_T/\lambda_{\rm KK}$. For $\theta = 130^\circ$ (as for $LaMnO_3$, Fig. 4) we find $T^{\varepsilon_T}_{\rm KK} \sim 0.84 T^0_{\rm KK}$ and $2|\Delta E|/k_B T^{\varepsilon_T}_{\rm KK} \sim 0.15$. This ratio is in qualitative agreement with what we find with DMFT for $LaMnO_3$, $|\Delta E| \sim 10$ meV.